

# On the Development of Superconducting Microstrip Filters for Mobile Communications Applications

Jia-Sheng Hong, *Member, IEEE*, Michael J. Lancaster, *Member, IEEE*, Dieter Jedamzik, and Robert B. Greed

**Abstract**—This paper presents recent developments of an eight-pole planar high-temperature superconducting (HTS) bandpass filter with a quasi-elliptic function response. A novel planar filter configuration that allows a pair of transmission zeros to be placed at the band edges is described. The miniature HTS filter has a fraction bandwidth less than 1% and is designed for mobile communication base-station applications to increase sensitivity and selectivity. Design considerations including filter characteristics, design approach, sensitivity analysis and unloaded quality factor of resonators are addressed. The filter was fabricated using double-sided YBCO thin film on an MgO substrate of size  $0.3 \times 22.5 \times 39$  mm. Very good experimental results were obtained with the filter cooled using liquid nitrogen. The minimum passband loss was measured to be approximately 1 dB. The passband width at points 1 dB down from the minimum loss point was 12.8 MHz for a center frequency of 1738.5 MHz. High selectivity was achieved with a 30-dB rejection bandwidth of 16 MHz.

**Index Terms**—Microstrip filters, mobile communication systems, superconducting filters.

## I. INTRODUCTION

THERE IS currently considerable interest in using high-temperature superconducting (HTS) materials for the construction of high-performance filters for mobile communication applications [1]–[11]. System benefits to the cellular mobile communications through the application of HTS technology focus on increased sensitivity and selectivity. Increased sensitivity increases the radio coverage. Hence, the number of base transceiver stations (BTS's) and the investment necessary to secure the radio coverage of a given area will be reduced. This is obviously paramount in rural areas. In urban interference-limited areas, increased sensitivity allows the mobile terminals to reduce the average radiated power and increase their autonomy for a given battery capacity. This may also have potential environmental and health benefits. Increased selectivity reduces out-of-band interference and, thus, is able to better utilize the frequency spectrum for mobile communications. This is highly desirable since the soaring demand for mobile communications place severe demands on the frequency resources as the allocated bandwidth becomes increasingly congested.

Manuscript received June 5, 1998. This work was supported by the European Commission under the Superconducting Systems for Communications Project. The work of M. J. Lancaster was supported by the Nuffield Foundation.

J.-S. Hong and M. J. Lancaster are with the School of Electronic and Electrical Engineering, University of Birmingham, Edgbaston, Birmingham B15 2TT, U.K.

D. Jedamzik and R. B. Greed are with GEC-Marconi Research Centre, Great Baddow, Chelmsford Essex CM2 8HN, U.K.

Publisher Item Identifier S 0018-9480(99)06591-6.

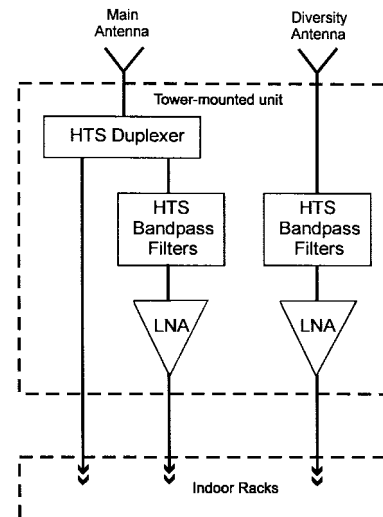


Fig. 1. Typical base-station sector using HTS subsystem.

HTS receiver bandpass filters play an essential role in achieving high sensitivity and selectivity in a base-station receiver system. In this paper, we report on the development of a novel HTS bandpass filter for a European mobile communications system. The receiver filter was for the DCS1800 standard, which covers the frequency range of 1710–1785 MHz. The block diagram is shown in Fig. 1. The filter was designed to cover a 15-MHz sub-band of this frequency range, providing low insertion loss and very steep rolloff at the filter band edges. This filter was developed within a European consortium sponsored by the European Commission. It involved a number of companies (GEC-Marconi, Great Baddow, Chelmsford Essex, U.K., Thomson CSF, Gennevilliers, France, and Lybold, Koln, Germany) and two Universities (Birmingham University, Edgbaston, Birmingham, U.K. and Wuppertal University, Wuppertal, Germany). The project acronym is SUCOMS, which stands for superconducting systems for communications, and it is funded through the Advanced Communications Technologies and Services (ACTS) Program. The objective of the project was to construct a HTS-based transceiver for mast-mounted DCS1800 base stations. The filter described here is one of two designs for front-end filtering on the receive side. More details of the project can be found in [9]–[11].

## II. FILTER CHARACTERISTICS

In general, there are different types of filter characteristics, (e.g., Chebyshev, Butterworth, etc.) and a bandpass filter may be designed to have any one of them. Therefore, it is important

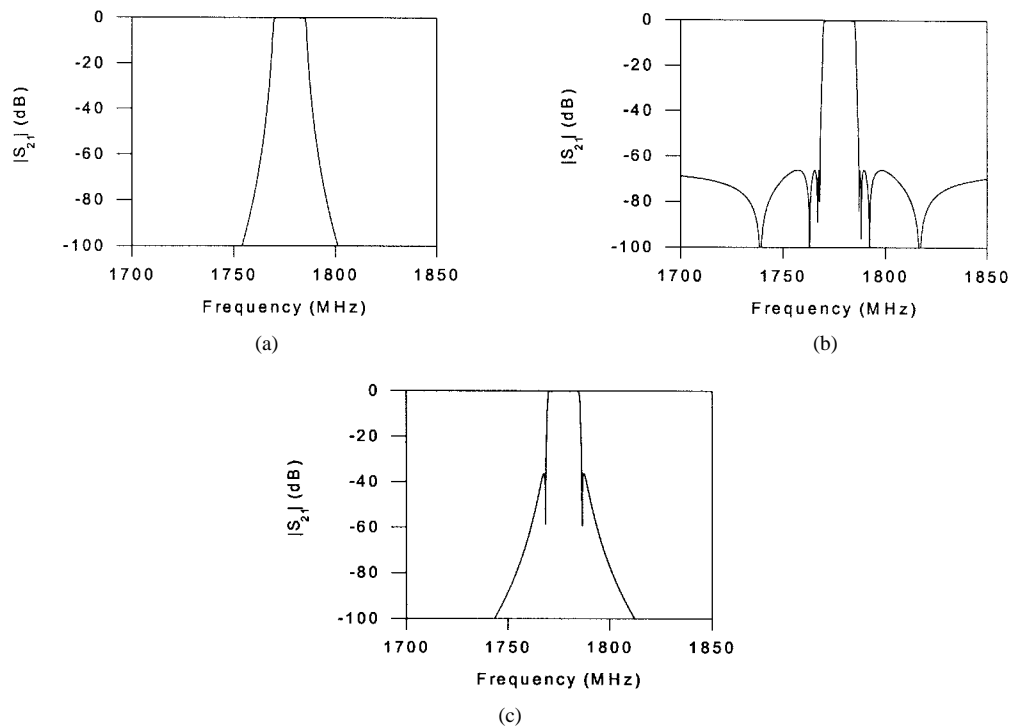


Fig. 2. Typical transmission characteristics of three types of eight-pole bandpass filters. (a) Chebyshev. (b) Elliptic function. (c) Quasi-elliptic function.

to assess the performance of different types of bandpass filters against the preliminary specification for the preselect bandpass filters to be integrated in the subsystem of Fig. 1. This helps to identify the optimum type and the degree of filter to meet the specification. For this purpose, we have studied three types of filters, namely: 1) Chebyshev; 2) quasi-elliptic; and 3) elliptic function filters against the following simplified specification:

center frequency	1777.5 MHz;
passband width	15 MHz;
passband insertion loss	$\leq 0.3$ dB;
passband return loss	$\leq -20$ dB;
30-dB rejection bandwidth	17.5 MHz;
transmit band rejection	$\geq 66$ dB (1805–1880 MHz).

Fig. 2 shows typical transmission characteristics of the three types of the filters. As can be seen, the distinguished differences among them are the locations of transmission zeros. While the Chebyshev filter has all transmission zeros at dc and infinite frequencies, the elliptic function filter has all transmission zeros at finite frequencies and exhibits an equal ripple at the stopband. The quasi-elliptic function filter concerned here has only a single pair of transmission zeros at finite frequencies, with the remainders at dc and infinite frequencies. From this study, the following conclusions can be drawn on the applicability of the filter types considered.

- 1) Filters with a low number of poles require a lower  $Q$  to meet the passband insertion specification. It is estimated the  $Q$  that can be attained is 50 000. Therefore, provided the required rejection and selectivity can be met, a filter with as low a number of poles as possible should be used.
- 2) The insertion loss at the passband edge as well as at midband must be considered. The loss at the band edge

is more predominant in the elliptic and quasi-elliptic function filters due to the effect of transmission zero near the cutoff frequency.

- 3) The Chebyshev filter with the same number of poles as an elliptic or quasi-elliptic function filter has poorer selectivity close to the passband edge, though it has better rejection at the transmit band (see Fig. 2). Increasing the number of poles can improve selectivity, but the penalty is an increased passband insertion loss (see Fig. 3). The Chebyshev filter is unsuitable for the SUCOMS requirement, in which a very high selectivity is required.
- 4) For a given number of poles, an elliptic function filter has higher selectivity close to the passband edge, but poorer rejection in the transmit band compared with a quasi-elliptic function filter (see Fig. 2).
- 5) The elliptic function filter is difficult to implement using distributed elements. An eight-pole quasi-elliptic function provides the best solution to meet the SUCOMS specification.

### III. FILTER CONFIGURATION

Having decided the filter type and degree, we have developed the novel microstrip filter configuration shown in Fig. 4 for realization of the quasi-elliptic function response. The filter is comprised of eight microstrip meander open-loop resonators. The attractive features of this filter are not only its small and compact size, but also its capability of allowing a cross coupling to be implemented such that a pair of transmission zeros (or attenuation poles) at finite frequencies can be realized. A general coupling structure for the quasi-elliptic filter is depicted in Fig. 5, where each node represents

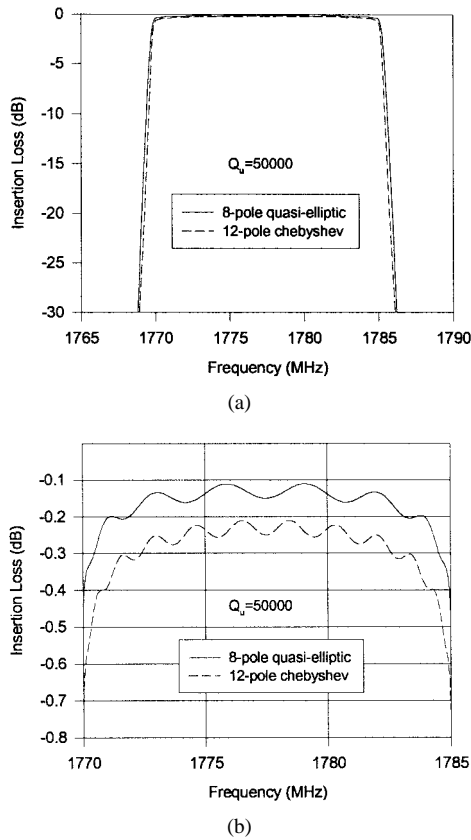


Fig. 3. Comparison of 12-pole Chebyshev and eight-pole quasi-elliptic function filters that meet the selectivity (a 30-dB rejection bandwidth of 17.5 MHz).

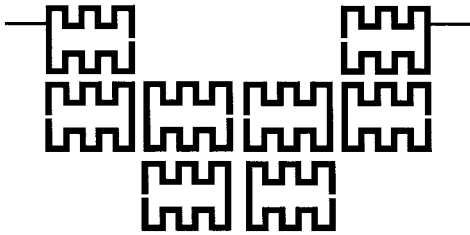


Fig. 4. Eight-pole microstrip filter configuration for HTS thin-film implementation.

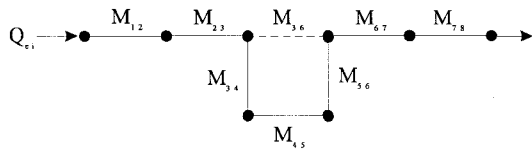


Fig. 5. A general coupling structure of the microstrip filter of Fig. 4.

a resonator, the full lines indicate the main path couplings, and the broken line denotes the cross coupling. It is important that the sign of cross coupling  $M_{36}$  is opposite to that of  $M_{45}$  in order to realize a pair of attenuation poles at finite frequencies. This simply implies that  $M_{36}$  and  $M_{45}$  are out-phase.

#### IV. FILTER DESIGN

The filter was synthesized against the specification starting from a low-pass prototype filter, as shown in Fig. 6, where

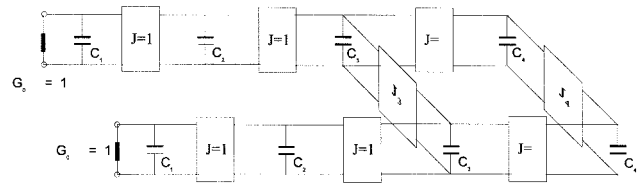


Fig. 6. Low-pass prototype for the filter synthesis.

$J$  is the characteristic admittance of the inverter and  $C$  is the capacitance. The bandpass design parameters, namely, the inter-resonator coupling coefficients and the input-output external quality factors in Fig. 5 are then calculated by

$$\begin{aligned} M_{12} &= M_{78} = \frac{\text{FBW}}{\sqrt{C_1 C_2}} \\ M_{34} &= M_{56} = \frac{\text{FBW}}{\sqrt{C_3 C_4}} \\ M_{36} &= \frac{\text{FBW} \cdot J_3}{C_3} \\ M_{23} &= M_{67} = \frac{\text{FBW}}{\sqrt{C_2 C_3}} \\ M_{45} &= \frac{\text{FBW} \cdot J_4}{C_4} \\ Q_{ei} &= Q_{eo} = \frac{C_1}{\text{FBW}} \end{aligned} \quad (1)$$

where “FBW” signifies the fractional bandwidth of the band-pass filter. The synthesis, which is nontrivial [12], yields the element values of the low-pass prototype

$$\begin{aligned} C_1 &= 1.02940 \\ C_3 &= 1.99314 \\ J_3 &= -0.40624 \\ C_2 &= 1.47007 \\ C_4 &= 1.96885 \\ J_4 &= 1.43484. \end{aligned} \quad (2)$$

For fractional bandwidth,  $\text{FBW} = 0.00844$  in our case, substituting (2) into (1) gives

$$\begin{aligned} M_{12} &= M_{78} = 0.00686 \\ M_{34} &= M_{56} = 0.00426 \\ M_{36} &= -0.00172 \\ M_{23} &= M_{67} = 0.00493 \\ M_{45} &= 0.00615 \\ Q_{ei} &= Q_{eo} = 121.98281. \end{aligned} \quad (3)$$

The theoretical response of the filter based on the low-pass prototype is plotted in Fig. 7 against the specifications (see gray lines).

The physical dimensions of the filter were determined using a full-wave electromagnetic (EM) simulator that simulated the coupling coefficients and external quality factors against physical structures, as described in [13] and [14]. Fig. 8 shows the computed frequency response of the final filter using full-wave analysis software.<sup>1</sup> Note that due to the complexity of

<sup>1</sup>EM User's Manual, Sonnet Software Inc., New York, 1993, version 2.4.

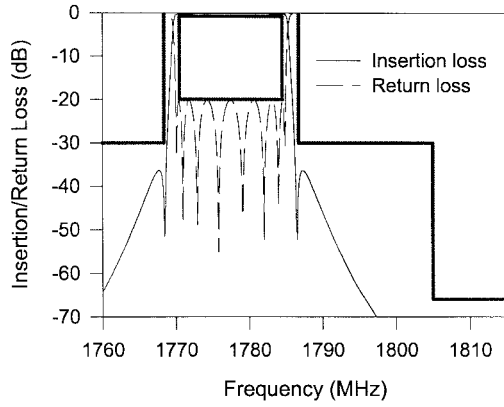


Fig. 7. Theoretical performance of the designed filter against the specifications (gray lines).

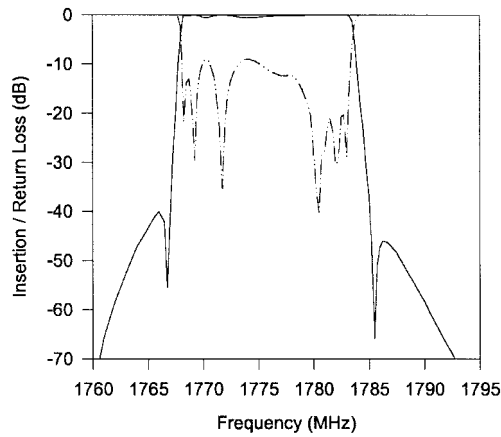


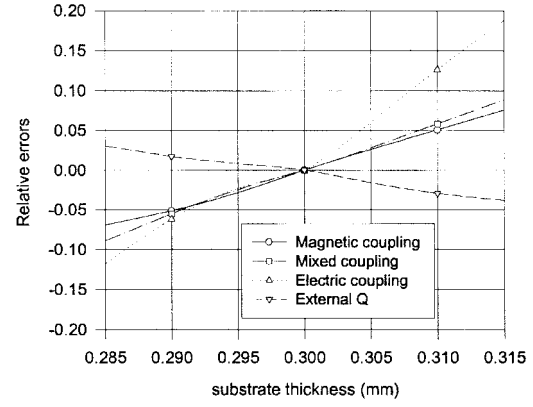
Fig. 8. Full-wave EM simulated performance of the designed filter.

the filter structure, a cell size of 0.05 mm was used. This means that the filter dimensions entered for the simulation were rounded off to a precision of 0.05 mm. Nevertheless, the full-wave simulated response did verify the design approach.

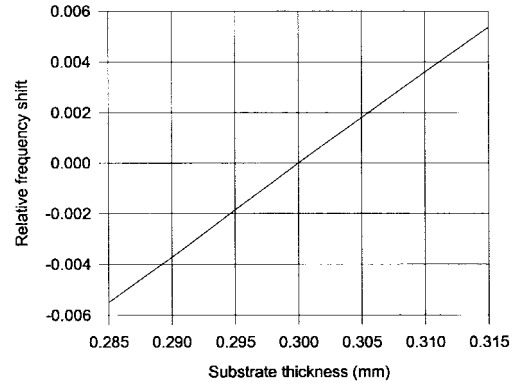
## V. SENSITIVITY ANALYSIS

The sensitivity analysis is very important for the filter design, particularly for the filter tuning, mainly because of fabrication errors. Among several possible error sources, we have identified that the thickness of the substrates used is a main source. The tolerance of substrate thickness is  $\pm 5\%$ . This tolerance is not only applied to the different substrates, but also to the variation of the thickness of a single substrate. This is a more serious problem for narrow-band filters.

Fig. 9(a) shows how the change of substrate thickness causes the change of the couplings and external quality factor. These typical results were obtained from the full-wave EM simulations. Note that the normal substrate thickness is 0.3 mm, as specified by the design. As can be seen when the substrate thickness varies in a range of  $0.3 \pm 5\%$  mm, the relative errors of the couplings and external quality factor with respect to that for the normal substrate thickness are within  $\pm 10\%$ , except for the electric coupling, which has a relative error ranging from  $-12\%$  to  $+18\%$ . The resonant frequency of microstrip meander open-loop resonators also depends on



(a)



(b)

Fig. 9. (a) Simulated relative errors of the couplings and external quality factor against the substrate thickness. (b) Simulated relative frequency shift of microstrip meander open-loop resonators against the substrate thickness.

the substrate thickness. The simulated relative frequency shift with respect to the resonant frequency on a 0.3-mm-thick MgO substrate, as shown in Fig. 9(b), is within  $\pm 0.6\%$ . This, however, results in approximately  $\pm 10$ -MHz frequency shift from a normal resonant frequency of 1777.5 MHz. This amount of frequency shifting is obviously not acceptable for a 15-MHz bandwidth filter. It may be interesting to point out that the meander open-loop resonator is more dependent on the substrate thickness than the straight half-wavelength resonator, which shows only  $\pm 0.25\%$  frequency shift in the same range of substrate thickness. This is because of the effect of discontinuities (right-angle bends) along the meander open-loop resonator.

Having quantified the effect of the variation of substrate thickness on the couplings, external quality factor, and resonant frequency, we further carried out the sensitivity analysis to see the effect of the change of design parameters on the filter response. The results are shown in Figs. 10 and 11, where each diagram shows the effect of one parameter. We can immediately see that the effect of the frequency shift is much more significant. This indicates that the frequency tuning is more important.

## VI. QUALITY-FACTOR OF RESONATORS

It is important to evaluate the achievable unloaded quality factor  $Q_u$  of the HTS resonators used in the filter. This will

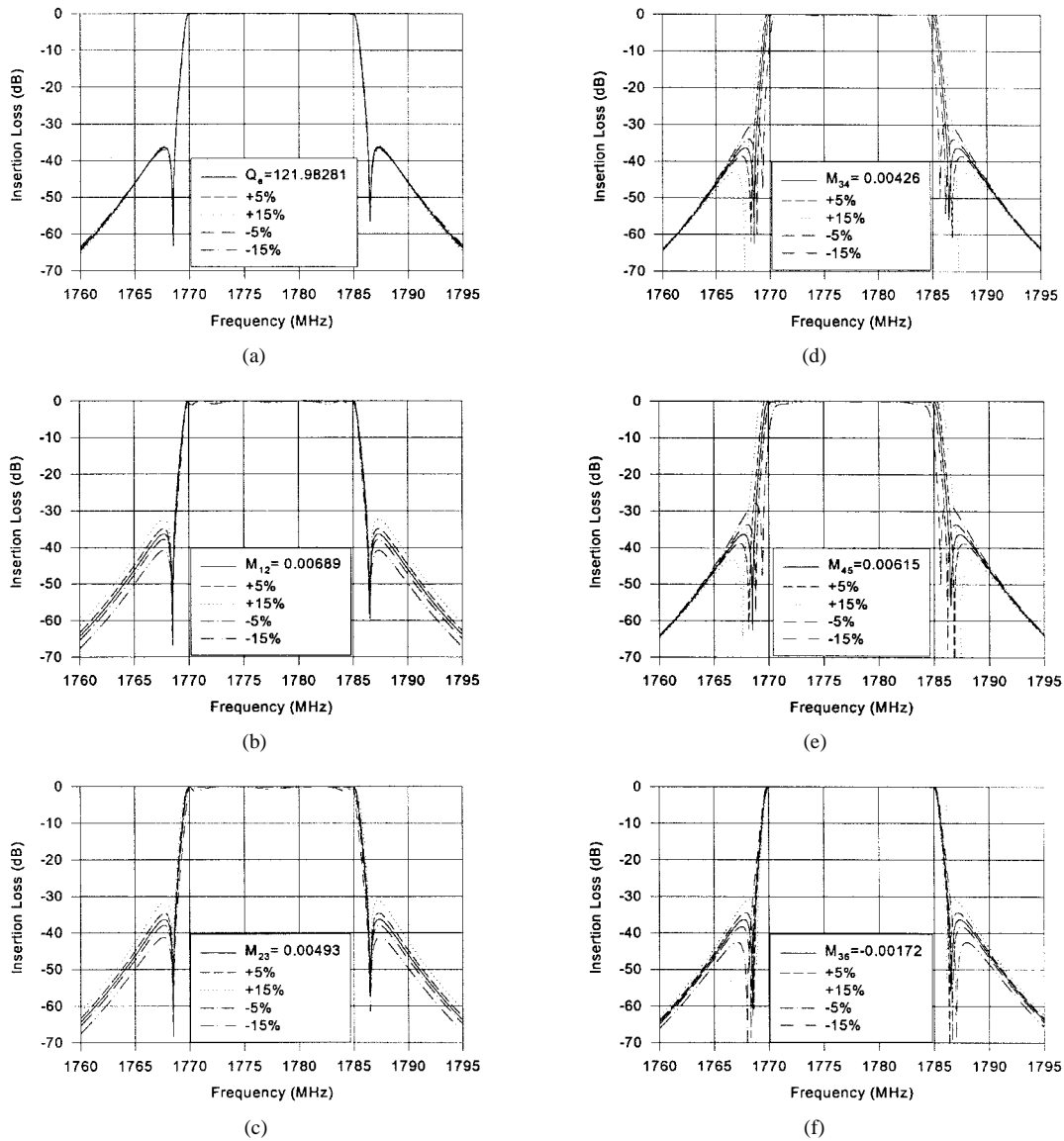


Fig. 10. The change of filter frequency response against the change of the external quality factor and coupling coefficients.

serve as a justification whether or not the required insertion loss of the bandpass filter can be met. Three loss mechanisms should usually be considered for evaluation of  $Q_u$ . They are the losses associated with the HTS thin film, the dielectric substrate, and the package housing made out of a normal conductor, respectively. Therefore, the unloaded quality factor  $Q_u$  can be found from

$$\frac{1}{Q_u} = \frac{1}{Q_c} + \frac{1}{Q_d} + \frac{1}{Q_h} \quad (4)$$

where  $Q_c$  is the quality factor of the HTS thin-film microstrip resonator,  $Q_d$  is the quality factor of the dielectric substrate, and  $Q_h$  is the quality factor of the package housing. Calculations of these quality factors are nontrivial because they require the knowledge of EM field distributions that depend on the geometry of microstrip resonator, the size of housing, and the boundary conditions imposed. Nevertheless, the following considerations are useful as guidelines for the filter design.

Assuming a uniform field between the microstrip and its ground plane, it can be shown that the quality factor of the

HTS microstrip resonator with a HTS ground plane (normally, an HTS ground is needed to achieve a higher  $Q_u$ ) may be estimated by [4]

$$Q_c \approx \pi \frac{h}{\lambda} \frac{\eta_0}{R_s} \quad (5)$$

where  $h$  is the substrate thickness,  $\lambda$  and  $\eta_0 (\approx 377 \Omega)$  are the wavelength and wave impedance in free space, and  $R_s$  is the surface resistance of the HTS thin film. It is commonly accepted that the surface resistance of the HTS thin film is proportional to  $f^2$  with  $f$  being the frequency. Thus, the  $Q_c$  is actually proportional to wavelength or inversely proportional to frequency. Having a thick substrate can increase the  $Q_c$ , but care must be taken because this increases the radiation and unwanted couplings as well. At a frequency of 2 GHz and a temperature of 60 K,  $R_s \leq 10^{-5} \Omega$  can be expected for a good YBCO thin film. If we let  $h = 0.3$  mm,  $\lambda = 150$  mm, and  $R_s = 10 \mu\Omega$ , we then find that  $Q_c \approx 240\,000$ .

The dielectric loss can be taken into account in terms of a complex permittivity of the dielectric substrate  $\epsilon = \epsilon' - j\epsilon''$

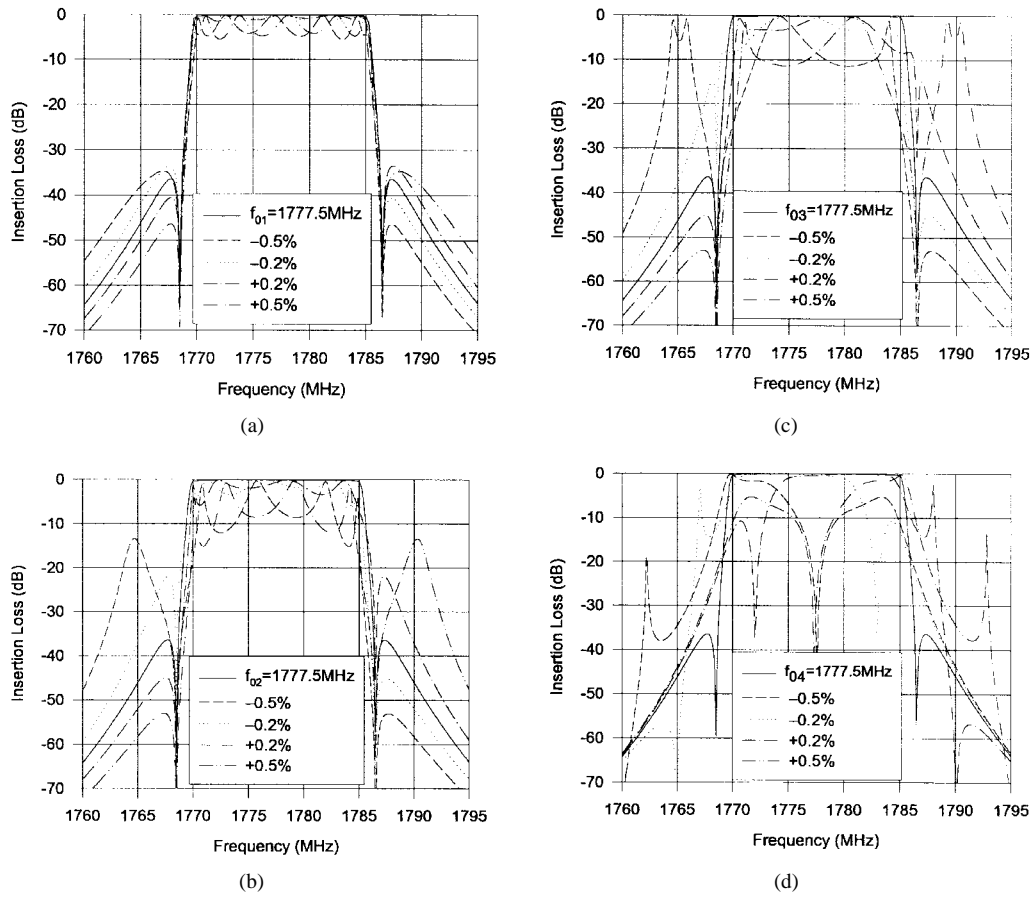


Fig. 11. The change of filter frequency response against the frequency shift of resonators.

with the negative imaginary part denoting energy loss [15]. Hence, the loss in a dielectric substrate may be attributed to an effective conductivity  $\omega\epsilon''$ . It can be shown that

$$Q_d \geq \frac{\epsilon'}{\epsilon''} = \frac{1}{\tan \delta}. \quad (6)$$

For MgO substrates, the typical value of  $\tan \delta$  is the order of  $10^{-5}$  to  $10^{-6}$  for a temperature ranging from 80 to 40 K [16], [17]. Therefore, at an operation temperature of 60 K and frequency of approximately 2 GHz, we can expect that  $Q_d > 10^5$  for MgO substrates.

The power loss of the housing due to nonperfect conducting walls at resonance may be expressed as

$$P_h = \frac{R_h}{2} \int |\underline{n} \times \underline{H}|^2 dS. \quad (7)$$

Here,  $R_h$  is the surface resistance of the housing walls,  $\underline{n}$  is the unit normal to the housing walls, and  $\underline{H}$  is the magnetic field at resonance. The housing walls are normally gold-plated to a thickness that is thicker than the skin depth. Although the surface resistance of gold is about two orders larger than that of the HTS thin film, the fields intercepted by the housing walls, which are normally located within the near-field region of the resonator, are weaker because they actually decay very fast, proportionally to  $1/r^3$  (static field) or  $1/r^2$  (induced field), where  $r$  is the distance from the HTS thin-film resonator. Therefore, the housing quality factor  $Q_h$ , which is inversely proportional to  $P_h$  of (7), can generally reach a higher value

with a larger housing size. Alternatively, one could optimize the shape of a resonator or use a lumped resonators to confine the fields in the substrate to obtain a higher  $Q_h$ , which may, however, reduce  $Q_c$ . If we assume  $Q_c = Q_d = 150\,000$ , we need a  $Q_h$  of 15 000 as well to achieve an unloaded quality factor  $Q_u$  of 50 000 according to (4). For system cooling and assembling, a smaller filter housing is usually desirable. If the small housing does cause a problem associated with the housing loss, an effective approach to increase the housing quality factor is to increase the housing size, particularly its height. By doing so, one must be careful about any housing mode that might be excited.

In order to find the unloaded quality factor experimentally, a single HTS microstrip meander open-loop resonator was fabricated using double-sided YBCO thin films on an MgO substrate with a size of 12 mm  $\times$  10 mm  $\times$  0.3 mm. The resonator was fixed on a gold-plated titanium carrier and assembled in a package housing for the filter. The inner area of the housing is 39.2  $\times$  25.6 mm with a distance of 3 mm from the substrate to the housing lid. Two copper microstrip feed lines were inserted between the HTS resonator and the input–output (I/O) ports on the housing to excite the HTS resonator. The loaded quality factor  $Q_L$  was measured using an HP8720A network analyzer. The unloaded quality factor is extracted by  $Q_u = Q_L/(1 - |S_{21}|)$  with  $|S_{21}|$  being the magnitude of an  $S$ -parameter measured at the resonant frequency. The results of  $Q_u$  obtained at a different

TABLE I  
MEASURED UNLOADED QUALITY FACTOR OF THE HTS MICROSTRIP MEANDER  
OPEN-LOOP RESONATOR

Temperature	45 K	50 K	60 K	70 K	77 K
$Q_u$	56900	50766	47300	38800	25400

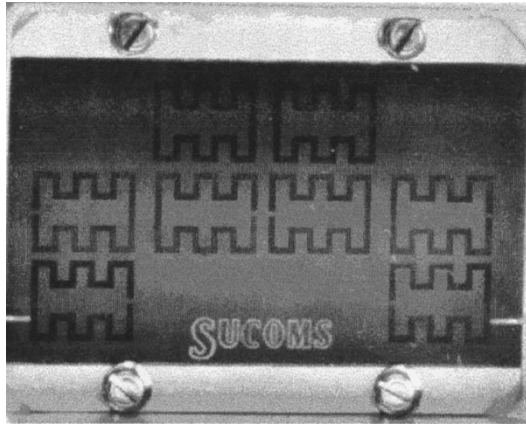


Fig. 12. Fabricated HTS quasi-elliptic function filter using microstrip meander open-loop resonators.

temperature are shown in Table I. As can be seen, the unloaded quality factor is very close to 50 000 at 60 K.

## VII. FILTER FABRICATION AND MEASUREMENT

The superconducting filter was fabricated using  $\text{YBa}_2\text{Cu}_3\text{O}_7$  thin-film HTS material. This was deposited onto both sides of a MgO substrate that was  $0.3 \times 39 \times 22.5$  mm and had a dielectric constant of 9.65. Fig. 12 is a photograph of the fabricated HTS bandpass filter assembled inside the housing. The size of the packaged filter is 2 in  $\times$  1.5 in  $\times$  0.5 in; considerably smaller than similar filters using any other technology.

The packaged superconducting filter was fixed on a copper bar that was immersed in liquid nitrogen as a cool base, while the filter was kept above the surface of liquid nitrogen for tuning. Hence, the temperature on the filter was actually higher than 77 K. The tuning is necessary because of a variation in substrate thickness, which has a considerable impact on the performance of narrow-band filters, as mentioned before. To tune the filter, the package for the filter has 16 tuning screws appropriately positioned. The filter was measured using the HP8720 network analyzer. Fig. 13 shows preliminary experimental results after tuning. The filter shows the characteristic of the quasi-elliptical response with two diminishing transmission zeros near the passband edges. The minimum passband loss was measured to be approximately 1 dB. The passband width at points 1 dB down from the minimum loss point was 12.8 MHz for a center frequency of 1738.5 MHz. The two transmission zeros resulted in a sharper filter skirt so as to improve the selectivity of the filter. The measured 30-dB rejection bandwidth was 16 MHz. The wider band response is plotted in Fig. 14, showing that spurious responses do not occur up until approximately 3 GHz. This stopband range is more than adequate for our applications. This filter was designed for the receiver and was required to handle a maximum input power of 0 dBm. Experimentally, it was found

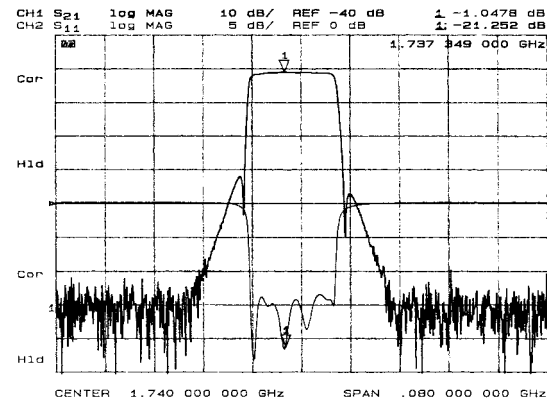


Fig. 13. Frequency response of the HTS quasi-elliptic function bandpass filter.

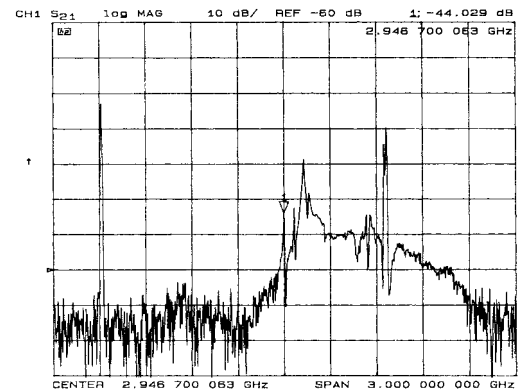


Fig. 14. Spurious response of the filter.

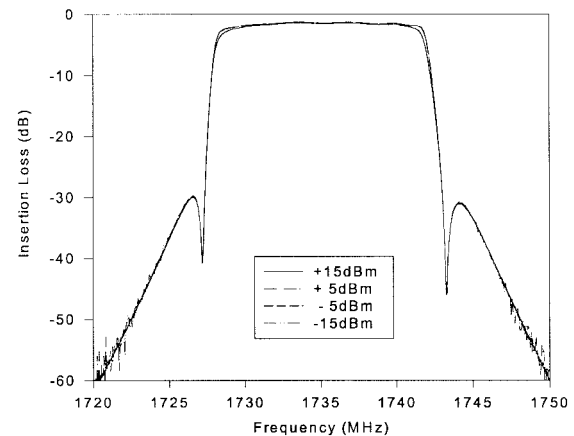


Fig. 15. Power dependence measurement of the filter.

that even for an input power of 5 dBm, the frequency responses of the filter did not change, as shown in Fig. 15.

Although very good experimental results have been obtained, some specifications (as referring to Fig. 7) have not been met with this filter that resulted from the first iteration of the design. It was found that the substrate used for this filter had a thickness actually thinner than 0.3 mm, as required by the design. This might cause a lower center frequency and a smaller passband bandwidth as measured. Both the center frequency and passband bandwidth would be expected to be corrected in the next iteration of the design. The measured insertion loss was higher than that expected from the measured unloaded quality factor of the single resonator at 77 K, as

described in Section VI. For a  $Q_u$  of 25 400 at 77 K, the minimum loss would be expected to be approximately 0.3 dB. The higher insertion loss of the filter would first attribute to the non-HTS parts of the filter. The housing used to test the filter included normal-metal connectors, silver-plated feed lines (each 2-cm long) at the input and output of the filter, and silver epoxy contacts made between the connectors and silver-plated feed lines. In addition, because the filter was kept above the surface of liquid nitrogen for tuning and the temperature on the filter was actually higher than 77 K as mentioned above, the  $Q_u$  would be lower than 25 400, increasing the insertion loss. Finally, it should be mentioned that the single resonator used to evaluate the  $Q_u$  and the HTS filter were made on different wafers. There might be a discrepancy in the HTS film quality as well.

## VIII. CONCLUSION

We have presented recent developments of an eight-pole planar HTS bandpass filter with a quasi-elliptic function response within an European research project of SUCOMS. We have introduced a novel filter configuration that allows a single pair of transmission zeros to be realized and miniatures the size of filter. Design considerations including the filter characteristics, design approach, sensitivity analysis, and unloaded quality factor of resonators have been addressed. The filter was fabricated using double-sided YBCO thin film on an MgO substrate of size 0.3 mm × 22.5 mm × 39 mm. It is shown that the excellent performance and small size of the filter presented make it hold promise for mobile communications application.

## REFERENCES

- [1] D. Reeder, "A cryogenic option for expanding coverage," in *Mobile Commun. Int. (SCT)*, June 1996, pp. 57–60.
- [2] STI Inc., "A receiver front end for wireless base stations," *Microwave J.*, vol. 39, no. 4, pp. 116–120, 1996.
- [3] R. B. Hammond, "HTS wireless filters: Past, present and future performance," *Microwave J.*, vol. 41, no. 10, pp. 94–107, 1998.
- [4] M. J. Lancaster, *Passive Microwave Device Applications of Superconductors*. Cambridge, U.K.: Cambridge Univ. Press, 1997.
- [5] S. H. Talisa, M. A. Robertson, B. J. Meler, and J. E. Sluz, "Dynamic range considerations for high-temperature superconducting filter applications to receive front ends," in *IEEE MTT-S Int. Symp. Dig.*, 1997, pp. 997–1000.
- [6] D. Zhang, G.-C. Liang, C. F. Shih, Z. H. Lu, and M. E. Johansson, "A 19-pole cellular bandpass filter using 75-mm diameter high-temperature superconducting films," *IEEE Microwave Guided-Wave Lett.*, vol. 5, pp. 405–407, Nov. 1995.
- [7] G.-C. Liang, D. Zhang, C. F. Shih, R. S. Withers, M. E. Johansson, D. E. Oates, A. C. Anderson, P. Polakos, P. Mankiewicz, E. Obaldia, and R. E. Miller, "High-power HTS microstrip filters for wireless communication," *IEEE Trans. Microwave Theory Tech.*, vol. 43, pp. 3020–3029, Dec. 1995.
- [8] G. Koepf, "Superconductors improve coverage in wireless networks," *Microwave RF*, vol. 37, no. 4, pp. 63–72, Apr. 1998.
- [9] M. J. Lancaster, J.-S. Hong, H. J. Chaplopka, D. Jedamzik, R. B. Greed, G. Auger, Y. Vourc'h, and J. C. Madge, "Superconducting filters for mobile communications base stations," in *ACTS Mobile Summit*, Aalborg, Denmark, Sept. 1997, pp. 150–155.
- [10] R. B. Greed, H. U. Haefner, and R. Mistry, "Cold communications in Europe," in *ACTS Mobile Summit*, Aalborg, Denmark, Sept. 1997, pp. 156–161.
- [11] Y. Vourc'h, G. Auger, H. J. Chaplopka, and D. Jedamzik, "Architecture of future basestations using high temperature superconductors," in *ACTS Mobile Summit*, Aalborg, Denmark, Sept. 1997, pp. 802–807.
- [12] J. D. Rhodes, "A low-pass prototype network for microwave linear phase filters," *IEEE Trans. Microwave Theory Tech.*, vol. MTT-18, pp. 290–301, Feb. 1970.
- [13] J.-S. Hong and M. J. Lancaster, "Couplings of microstrip square open-loop resonators for cross-coupled planar microwave filters," *IEEE Trans. Microwave Theory Tech.*, vol. 44, pp. 2099–2109, Nov. 1996.
- [14] ———, "Theory and experiment of novel microstrip slow-wave open-loop resonator filters," *IEEE Trans. Microwave Theory Tech.*, vol. 45, pp. 2358–2365, Dec. 1997.
- [15] R. E. Collin, *Foundations for Microwave Engineering*. New York: McGraw-Hill, 1992, ch. 2.
- [16] T. Konaka, M. Sato, H. Asano, and S. Kubo, "Relative permittivity and dielectric loss tangent of substrate materials for high- $T_c$  superconducting film," *J. Superconduct.*, vol. 4, no. 4, pp. 283–288, 1991.
- [17] J. Krupka, R. G. Geyer, M. Kuhn, and J. H. Hinken, "Dielectric properties of single crystals of  $\text{Al}_2\text{O}_3$ ,  $\text{LaAlO}_3$ ,  $\text{NdGaO}_3$ ,  $\text{SrTiO}_3$  and MgO at cryogenic temperatures," *IEEE Trans. Microwave Theory Tech.*, vol. 42, pp. 1886–1890, Oct. 1994.



**Jia-Sheng Hong** (M'94) received the D.Phil. degree in engineering science from Oxford University, Oxford, U.K., in 1994.

From 1979 to 1983, he was with Fuzhou University, as a Teaching/Research Assistant in radio engineering. From 1984 to 1985, he was with Karlsruhe University, Germany, where he was involved with microwave and millimeter-wave techniques. In 1986, he returned to Fuzhou University, as a Lecturer in microwave communications. In 1990 he was a graduate member of St. Peter's College, Oxford University, where he conducted research in EM theory and applications. Since 1994, he has been a Research Fellow at Birmingham University, Edgbaston, Birmingham, U.K. His current interests include RF and microwave devices for communications, microwave filters and antennas, microwave applications of high-temperature superconductors, EM modeling, and circuit optimization.

Dr. Hong was awarded a Friedrich Ebert Scholarship and a 1990 K. C. Wong Scholarship presented by Oxford University.



**Michael J. Lancaster** (M'91) received the physics degree and Ph.D. degree for research into nonlinear underwater acoustics from Bath University, Bath, U.K., in 1980 and 1984, respectively.

He then joined the Surface Acoustic Wave (SAW) Group, Department of Engineering Science, Oxford University, Oxford, U.K., as a Research Fellow, where his research was in the design of new novel SAW devices, including filters and filter banks. These devices worked in the frequency range of 10 MHz–1 GHz. In 1987, he became a Lecturer of EM theory and microwave engineering in the School of Electronic and Electrical Engineering, University of Birmingham, Edgbaston, Birmingham, U.K. Shortly after he joined the University of Birmingham, he began the study of the science and applications of high-temperature superconductors, working mainly at microwave frequencies. He currently heads the Electronic and Materials Devices Group as a Reader. His current personal research interests include microwave filters and antennas, as well as the high-frequency properties and applications of a number of novel and diverse materials.

Dr. Lancaster currently serves on the IEEE Microwave Theory and Techniques Society (MTT-S) International Microwave Symposium Technical Committee.

**Dieter Jedamzik**, photograph and biography not available at the time of publication.

**Robert B. Greed**, photograph and biography not available at the time of publication.